ISSN 0006-2979, Biochemistry (Moscow), 2006, Vol. 71, No. 10, pp. 1101-1109. © Pleiades Publishing, Inc., 2006.
Published in Russian in Biokhimiya, 2006, Vol. 71, No. 10, pp. 1360-1370.
Originally published in Biochemistry (Moscow) On-Line Papers in Press, as Manuscript BM05-277, July 2, 2006.

Comparative Study of Effects of Polyols, Salts, and Alcohols on Trichloroacetic Acid-Induced State of Cytochrome *c*

Aabgeena Naeem, Mohd. Tashfeen Ashraf, Mohd. Akram, and Rizwan Hasan Khan*

Interdisciplinary Biotechnology Unit, Aligarh Muslim University, Aligarh-202002, India;
fax: (91-571) 272-1776; E-mail: rizwanhkhan@hotmail.com; rizwanhkhan1@yahoo.com

Received January 23, 2006
Revision received April 18, 2006

Abstract—A systematic investigation of the effect of polyethylene glycols, salts, and alcohols on the trichloroacetic acid (TCA)-induced state of ferricytochrome *c* was made using various spectroscopic techniques. Native cytochrome *c* (Cyt *c*) has a fluorescence maximum at 335 nm, whereas the TCA-induced state of Cyt *c* has a red shift of 7 nm with enhanced fluorescence intensity. The near- and far-UV CD spectra showed a significant loss of tertiary and secondary structure, although the protein is relatively less unfolded as compared with a conformation at pH 2.0. Addition of 70% (v/v) polyols to TCA (3.3 mM)-induced state of Cyt *c* resulted in increased 1-anilino-8-naphthalene sulfonate binding and increased mean residue ellipticity at 222 nm, indicating increase in compactness with enhanced exposure of hydrophobic surface area. Also, the stabilizing effect of salts and alcohols on the TCA-induced state was studied and compared with their effect on trifluoroacetic acid-unfolded state of Cyt *c*. Among all the polyols, salts, and alcohols studied, PEG-400, $K_3[Fe(CN)_6]$, and butanol were the most efficient in inducing secondary structure in TCA-induced state as examined by the above-mentioned spectroscopic techniques. For salts, the efficiency in inducing the secondary structure followed the order $K_3[Fe(CN)_6] > KClO_4 > K_2SO_4 > KCl$. For alcohols, this order was found to be as follows: butanol > propanol > ethanol > methanol.

DOI: 10.1134/S0006297906100075

Key words: alcohol-induced state, anion-induced state, cytochrome *c*, circular dichroism, fluorescence, polyethylene glycol

Cytochrome *c* (Cyt *c*) is a small globular protein (104 amino acid residues, 12.7 kD) carrying a large component of basic residues. It has been widely used as a protein-folding model for kinetic as well as equilibrium studies. Fink et al. have classified Cyt *c* as type I protein based on its acid unfolding behavior [1-7]. At pH 2.2, ferricytochrome *c* is substantially unfolded at low ionic strength; upon addition of salts, the protein cooperatively folds to a compact structure, the A-state, which is stabilized by binding of anions to the positively charged groups on the protein surface [8, 9]. The A-state possesses α-helix structure comparable to that of the native state, but a fluctuating tertiary conformation [10, 11]. In particular, the hydrophobic core (containing the two major helices) and the heme group (stabilized by non-bonded interactions) are preserved in the A-state, while the loop regions are fluctuating and partly disordered. Of the two native axial ligands of the heme iron, only His18 is thought to remain coordinated to the heme iron in the A-state, while the Met80 axial bond is lost [12-14]. Goto and collaborators [14] have shown that the charge density of the anions is the main determinant that stabilizes the A-state; the higher the charge, the lower the ion concentration needed to induce formation of the molten globule. Santucci et al. [15] have suggested that small anions induce formation of a compact, highly structured state, in which the native Met80–Fe(III) axial bond is recovered and the native-like redox properties are restored.

In native horse heart Cyt *c*, bonds between the heme and four amino acids (Cys14, Cys17, His18, and Met80) anchor the heme and, together with an extensive array of noncovalent side-chain contacts, these bonds help to make the internal structure relatively rigid around the heme. The residues that are in van der Waals contact with heme are bulky hydrophobic groups that stabilize the structure and control the redox potential [16-21].

In earlier communications, we reported the effects of salts and alcohols on α-chymotrypsinogen, and the existence of molten globule states at low pH in bromelain and concanavalin A [22-25]. Effects of SDS and butanol at different pH values as well as effects of salts and alcohols on trifluoroacetic acid (TFA)-treated Cyt *c* have been

* To whom correspondence should be addressed.

studied at our laboratory [26, 27]. In the present study, we have investigated the effect of poly ethylene glycols (PEG-200 and PEG-400) on trichloroacetic acid (TCA)-induced state of Cyt *c*. TFA is a stronger denaturant than TCA, due to the presence of a fluorine group. A comparative study of the effect of salts and alcohols on TCA-induced state with TFA-induced state was also performed.

MATERIALS AND METHODS

Materials. Horse heart Cyt *c* (type III) was purchased from Sigma (USA). All the salts and alcohols used were procured from Qualigens (India). Reagents used were of analytical grade.

For studying the effects of polyols, salts, and alcohols on the TCA-induced state of Cyt *c*, it was incubated at room temperature for 1 h in the presence of different concentrations of polyols, salts, and alcohols.

Volumetric analysis. The concentration of trichloroacetic acid was determined by titration with 0.1 M Na_2CO_3 using methyl orange as indicator. The final concentration so obtained was 33 mM, which was then used to prepare 3.3 mM TCA in order to unfold Cyt *c* [28].

Soret-absorption spectroscopy. A Hitachi U-1500 single beam spectrophotometer was used to monitor the Soret absorption of the heme group at 410 nm, in a 10 mm pathlength cell. The concentration of native Cyt *c* was determined from the extinction coefficient of 106,000 $M^{-1}\cdot cm^{-1}$ at 410 nm.

Circular dichroism measurements. A JASCO J-720 spectropolarimeter calibrated with ammonium d-10-camphorsulfonate was used to measure circular dichroism. Protein concentration was 26 and 50 μM for far- and near-UV CD, respectively. The results were expressed as the mean residue ellipticity (MRE), which was calculated by the following formula:

$$MRE = \theta_{obs}/(10\cdot n\cdot C_p\cdot l)\ \text{mdeg}\cdot\text{cm}^2/\text{mol},$$

where θ_{obs} is the observed ellipticity in millidegrees, n is the number of amino acid residues, C_p is the molar concentration of Cyt *c*, and l is the length of the light path in cm.

C_m is defined as the midpoint of the transition at which half of the structure is induced in the presence of salts, polyols, and alcohols individually. From the MRE values obtained for the transition induced by salts and alcohols at fixed wavelength, the C_m values for respective salts and alcohols were calculated.

The α-helical content of Cyt *c* was calculated from the MRE value at 222 nm using the following equation as described by Chen et al. [29]:

$$\%\ \alpha\text{-helix} = (MRE_{222} - 2340)/30{,}300 \times 100.$$

Intrinsic fluorescence. The fluorescence spectra were recorded on a Shimadzu RF-540 spectrofluorimeter using a 10-mm quartz cell. Samples containing different concentrations of PEGs, salts, and alcohols were incubated at room temperature for 1 h before recording the tryptophan fluorescence. The excitation wavelength was 280 nm and the emission was recorded from 300 to 400 nm. The final protein concentration was 15 μM. For each sample, a proper blank was taken into consideration.

Extrinsic fluorescence measurements. A stock solution of 1-anilino-8-naphthalene sulfonate (ANS) was prepared in distilled water and the concentration was determined using an extinction coefficient of 5000 $M^{-1}\cdot cm^{-1}$ at 350 nm. The molar ratio of protein/ANS was 1 : 50. The excitation wavelength was at 380 nm and the emission spectra were recorded in the wavelength range 400 to 600 nm. The excitation as well as the emission slit width was 10 nm. The final protein concentration was 15 μM. It should be noted that organic solvents bind to

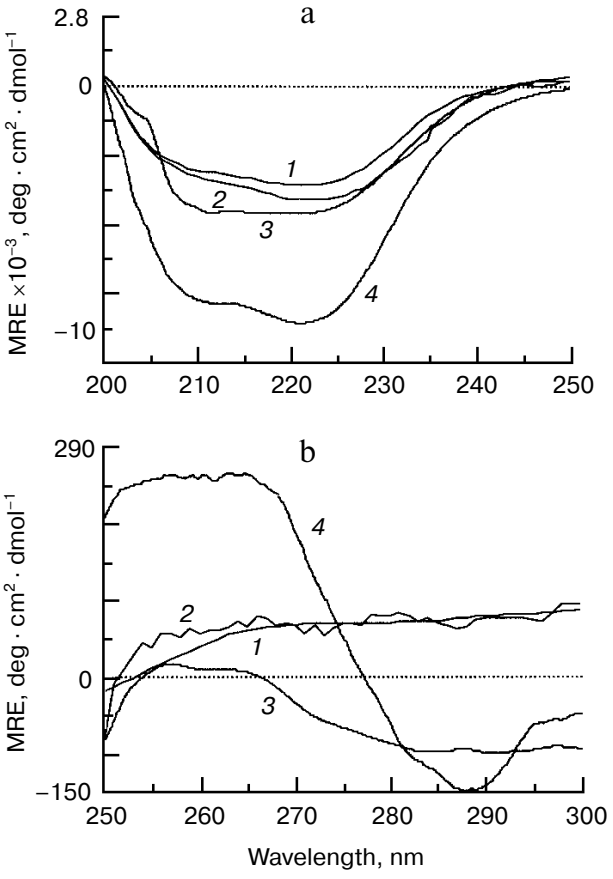

Fig. 1. Cyt *c* far-UV (a) and near-UV CD spectra (b): *1*) acid-unfolded state at pH 2.0, 10 mM glycine HCl buffer; *2*) 33 mM TCA-induced state; *3*) 3.3 mM TCA-induced state; *4*) native state at pH 7.0, 10 mM sodium phosphate buffer. Protein concentration was 26 (a) and 50 μM (b). The pathlength was 0.1 (a) and 1 cm (b).

ANS; therefore, to avoid anomaly, a proper blank was made for every point.

RESULTS

In order to examine the effect of TCA on secondary structure of Cyt *c*, the protein was titrated against trichloroacetic acid. Figure 1a shows the far-UV CD spectra of the native protein (curve *4*), Cyt *c* at pH 2.0 (curve *1*), Cyt *c* in 3.3 mM TCA (curve *3*), and Cyt *c* in 33 mM TCA (curve *2*). It was found that Cyt *c* at 3.3 mM TCA retains most of the secondary structure. Thus, it exists in a relatively compact state as compared to the state attained in 33 mM TCA (curve *2*) and at pH 2 (curve *1*), respectively (Fig. 1a). Near-UV CD spectra (Fig. 1b) show the loss of tertiary structure at 3.3 mM TCA (curve *3*) as compared that of native protein (curve *4*). The protein is relatively less unfolded as compared to 33 mM TCA (curve *2*) and at pH 2.0 (curve *1*). Thus, Cyt *c* at 3.3 mM TCA can be said to exist as a partially folded state with loss of tertiary structure. However, the presence of tertiary contacts cannot be ruled out.

Cyt *c* is a heme protein in which the resonance energy of the tryptophan excitation is transferred to the heme resulting in quenched tryptophan fluorescence with λ_{max} at 335 nm (Fig. 2a, curve *1*). A red shift of 7 nm is obtained in the TCA (3.3 mM)-induced state with enhanced fluorescence intensity (curve *2*). At pH 2.0, there was further enhancement in fluorescence intensity (curve *4*), and it was almost the same as in 33 mM TCA (Fig. 2a, curve *3*). In its native form, Cyt *c* showed negligible binding of ANS with emission maxima at 510 nm (Fig. 2b, curve *1*), which is characteristic of free ANS in water (Fig. 2b). The fluorescence intensity was maximal in the TCA-induced state (curve *4*) with a blue shift in emission maxima at 480 nm. Cyt *c* in 33 mM TCA (curve *3*) showed a decrease in fluorescence intensity followed by Cyt *c* at pH 2.0 (curve *2*) relative to that of 3.3 mM TCA. Henceforth, it is referred as the TCA-induced state.

Effect of polyethylene glycols on the TCA-induced state of Cyt *c*. *CD measurements.* Addition of PEG-200 and -400 to TCA-induced state of Cyt *c* up to 70% (v/v) led to an increase in helical content as evidenced by more negative MRE values at 208 and 222 nm. Figure 3a shows the far-UV CD spectra of TCA-induced state of Cyt *c* and

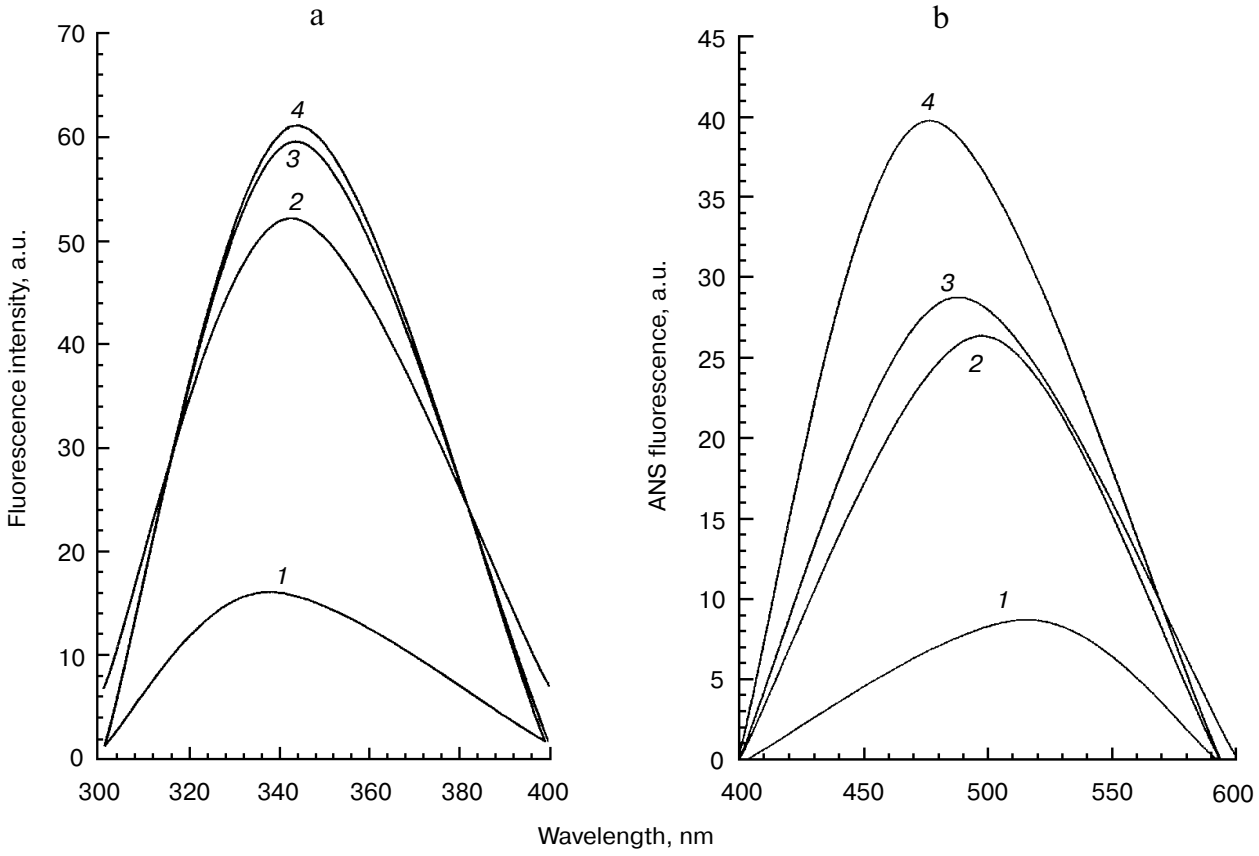

Fig. 2. Cyt *c* fluorescence spectra. a) Tryptophan fluorescence emission spectra of Cyt *c*: *1*) in 10 mM phosphate buffer, pH 7.0; *2*) in the presence of 3.3 mM TCA; *3*) in the presence of 33 mM TCA; *4*) acid-unfolded state at pH 2.0, 10 mM glycine-HCl buffer. b) ANS fluorescence emission spectra of Cyt *c*: *1*) in 10 mM phosphate buffer, pH 7.0; *2*) acid-unfolded state at pH 2.0, 10 mM glycine-HCl buffer; *3*) 33 mM TCA-induced state; *4*) in presence of 3.3 mM TCA. Protein concentration was 15 μM and pathlength was 1 cm.

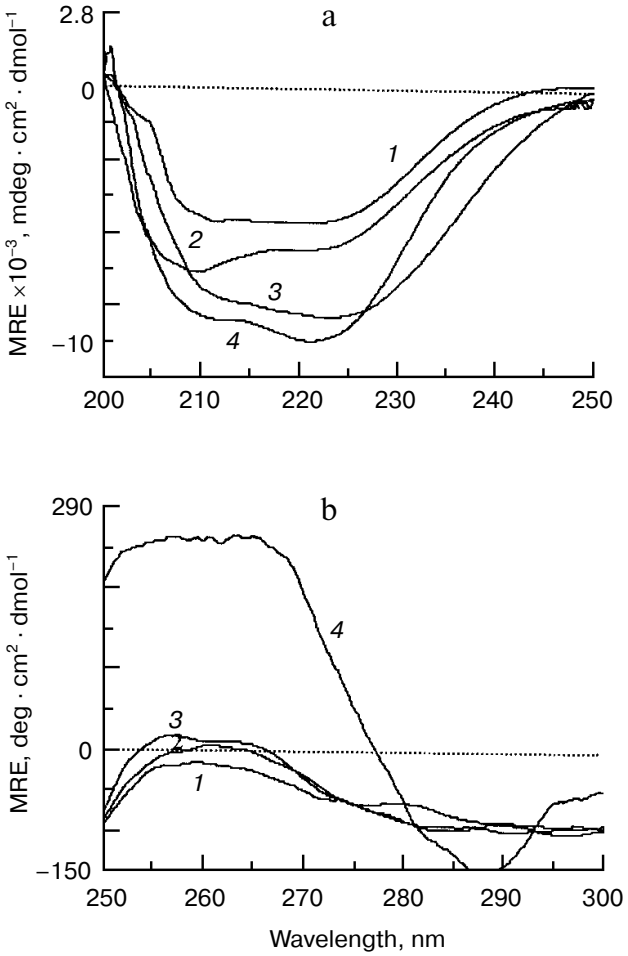

Fig. 3. CD spectra of the TCA-induced state of Cyt *c* in the presence of PEG. Far-UV CD spectra (a) and near-UV CD spectra (b) of Cyt *c* in the presence of 3.3 mM TCA (curve *1*) and at the respective maximum concentration of polyols, i.e. 70% PEG-200 (curve *2*) and 70% PEG-400 (curve *3*); curve *4* represents native protein. Protein concentration was 26 (a) and 50 μM (b) and pathlength was 0.1 (a) and 1 cm (b).

of native Cyt *c* and at the maximum concentrations of PEG-200 and -400. Curve *1* of Fig. 3a represents the far-UV CD spectra of Cyt *c* in the presence of 3.3 mM TCA. The spectrum of maximum concentration of PEG-200 (curve *2*) and PEG-400 (curve *3*), i.e. 70% (v/v), shows the negative increase in MRE. The CD spectra in the presence of 70% PEG-400 (curve *3*) approaches to native (curve *4*). The helical content calculated from the MRE value at 222 nm by the method of Chen et al. [29] for the native state at pH 7.0, and the TCA-induced state in the presence of 70% PE-400 was 26 and 28%, respectively. This is suggestive of an increase in secondary structural content (stabilization of α-helices). A summary of the respective maximum MREs at 222 nm in the presence of different concentrations of PEG-200 and -400, their C_m (the concentration of alcohol at which half of the structure is induced) values are given in Table 1. Figure 3b shows the near-UV CD spectra of TCA-induced state of Cyt *c* (curve *1*) in the presence of 70% PEG-200 (curve *2*) and PEG-400 (curve *3*) and native (curve *4*). The loss of signal in the near-UV CD region reveals the loss of tertiary contacts. Thus, an intermediate state in the presence of polyols is obtained at 70% (v/v). The PEG-200- and PEG-400-induced transition of TCA-induced state of Cyt *c* as observed in this study can be explained on the basis of enhanced hydrophobic interactions by addition of polyols, which are known to stabilize the helical structure of proteins. Such types of transitions have also been reported earlier for a number of proteins [10, 30, 31]. Formation of secondary structure in TCA induced state of Cyt *c* in the presence of polyols can be attributed to the greater number of OH groups as PEG-400 was found to be more effective than PEG-200. The effect of polyols increases with increasing concentration and number of OH groups [32].

Intrinsic tryptophan fluorescence. The intrinsic fluorescence maximum (λ_{max}) is an excellent parameter to monitor the polarity of tryptophan environment in the protein and is sensitive to the protein conformation [33]. Intrinsic fluorescence studies were performed to see the effect of PEGs on the conformation of the TCA-induced state of Cyt *c*. The absorption of PEG in the wavelength range used was duly taken into consideration. On addition of PEGs up to 70% to the TCA-induced state, enhancement in fluorescence intensity with a blue shift was observed (figure not shown for clarity). On addition of PEGs to the TCA-induced state, the tryptophan remains more exposed to the environment than it does in the native protein. Thus, as the concentration of PEGs is increased, the partially exposed tryptophan residue faces more and more nonpolar environment, explaining the blue shift and enhancement in tryptophan fluorescence. The increase was greater in PEG-400 than in PEG-200. This is possibly due to the presence of more hydroxyl groups in PEG-400 than PEG-200. An intermediate state in the presence of 70% PEGs on the TCA-induced state of Cyt *c* is obtained. A summary of tryptophan fluorescence intensity and emission maxima of native Cyt *c*, TCA induced state of Cyt *c*, and in the presence of PEGs is given in Table 2.

ANS fluorescence. Binding of ANS to hydrophobic regions of proteins has been widely used to study the folding intermediates formed during protein folding [34-37]. It should be noted that organic solvents change the properties of the environment; therefore, to avoid anomaly, a proper blank was made for every point. Table 2 summarizes the ANS fluorescence intensity and emission maxima of the TCA-induced state of Cyt *c*, in 70% PEG-200, 70% PEG-400, and the native protein. The intermediate state induced by polyols was further confirmed by extrinsic fluorescence studies (ANS binding). ANS fluorescence studies showed that 70% PEGs have the maximum ANS binding. Binding was maximum in PEG-400 fol-

Table 1. Midpoint of transition C_m, MRE_{222}, and helicity of the TCA-induced state of Cyt *c* under the influence of polyols, alcohols, and salts

Subject	C_m value***	Maximum MRE_{222}, deg·cm^2·dmol^{-1}	% α-helix**
Native Cyt *c*	n.d.*	−10.000	26
Polyols	**% (v/v)**		
PEG-200 (70% v/v)	23	−7.141	16
PEG-400 (70% v/v)	21	−9.112	22.4
Alcohols	**(M)**		
Methanol (14 M)	10.6	−6.000	12.1
Ethanol (12 M)	5.2	−6.201	12.7
Propanol (11 M)	4.8	−7.025	15.5
Butanol (9 M)	4.0	−7.410	17
Salts	**(mM)**		
$K_3[Fe(CN)_6]$ (1 mM)	0.6	−7.111	15.7
K_2SO_4 (10 mM)	4	−6.950	15.2
$KClO_4$ (20 mM)	9	−6.312	13.12
KCl (120 mM)	35	−6.113	12.5
TCA (3.3 mM)	n.d.*	−5.142	9.25

* n.d., not determined.
** Calculated by the method of Chen et al. [29].
*** C_m is defined as the midpoint of transition at which half of the structure is induced in the presence of salts, polyols, and alcohols individually.

Table 2. Fluorescence properties of the TCA-induced state of Cyt *c* under the influence of polyols, alcohols, and salts

Conditions	Intrinsic fluorescence		ANS fluorescence	
	intensity	emission maximum	intensity	emission maximum
TCA (3.3 mM)	52	345	40	480
Native	15	335	09	510
PEG-400 (70% v/v)	87	337	124	480
PEG-200 (70% v/v)	64	339	62	480
Butanol (9 M)	136	340	143	480
Propanol (11 M)	100	340	119	480
Ethanol (12 M)	82	342	107	490
Methanol (14 M)	64	342	87	490
$K_3[Fe(CN)_6]$ (1 mM)	24	339	59	480
K_2SO_4 (10 mM)	28	339	54	490
$KClO_4$ (20 mM)	32	340	51	490
KCl (120 mM)	38	342	46	490

lowed by PEG-200 and in TCA-induced state of Cyt *c*. Negligible binding was observed at pH 7.0. Hence, it can be concluded that at 70% PEG the TCA-induced state of Cyt *c* exists as the molten globule state.

Effect of salts on the TCA-induced state of Cyt *c*. *Effect of salts as studied by CD spectroscopy.* Figure 4a shows the far-UV CD spectra of the native protein and of the TCA-induced state of Cyt *c* in the presence of the

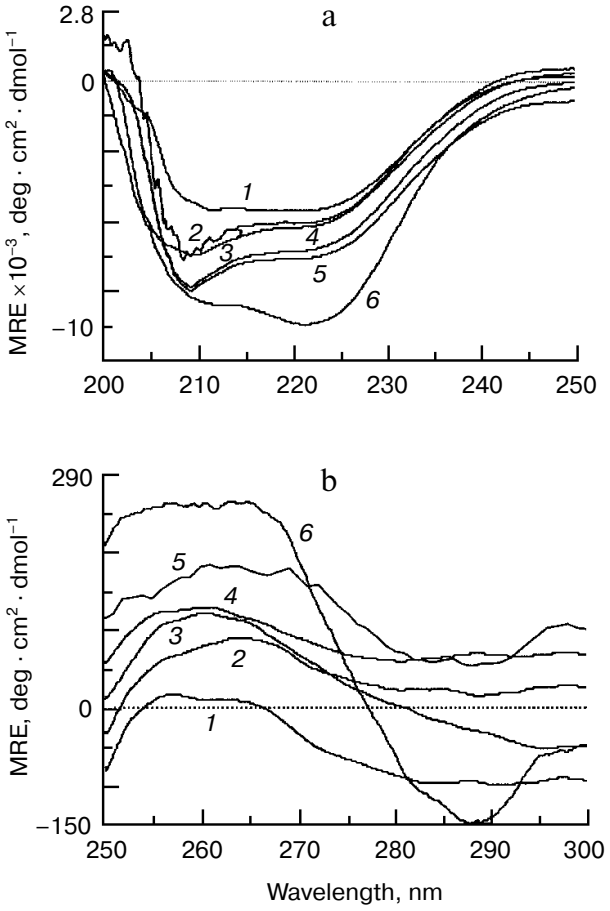

Fig. 4. Effect of salts on the TCA-induced state of Cyt *c*. Far-UV CD spectra (a) and near-UV CD spectra (b) of Cyt *c* in the presence of 3.3 mM TCA (curve *1*) and at the respective maximum concentration of salts, i.e., 1 mM $K_3[Fe(CN)_6]$ (curve *5*), 10 mM K_2SO_4 (curve *4*), 20 mM $KClO_4$ (curve *3*), 120 mM KCl (curve *2*), and native protein (curve *6*). Protein concentration was 26 (a) and 50 μM (b) and pathlength was 0.1 (a) and 1 cm (b).

respective maximum concentration of various salts. As can be seen from the figure, 1 mM $K_3[Fe(CN)_6]$ (curve *5*) shows the major changes in the spectra of the TCA-induced state of Cyt *c* (curve *1*) followed by 10 mM K_2SO_4 (curve *4*), 20 mM $KClO_4$ (curve *3*), and 120 mM KCl (curve *2*). A summary of the respective maximum MREs in the presence of salts, their C_m values, and percent α-helix is given in Table 1. The C_m value calculated for $K_3[Fe(CN)_6]$ was 0.6 mM, while for KCl it was 35 mM. At higher concentration of salts a compact secondary structure is formed. This state has comparable amounts of ordered secondary structure to that of the native protein (curve *6*) and can be termed as molten globule.

Figure 4b shows the near-UV CD spectra of native Cyt *c* (curve *6*), the TCA-induced state of Cyt *c* (curve *1*), and TCA-induced state of Cyt *c* in the presence of the respective maximum concentration of salts. As can be seen from the figure, the signal in the near-UV CD spectra in the presence of salts approaches the native state as compared to the TCA-induced and PEG-induced states (Fig. 3b). The maximum structural changes were induced by $K_3[Fe(CN)_6]$ (curve *5*) at lower concentration, as compared to K_2SO_4 (curve *4*), $KClO_4$ (curve *3*), and KCl (curve *2*). The effectiveness of anions in bringing about TCA-induced to molten globule transition in protein has been found to be consistent with the electronegativity series, representing the order of affinity of positively charged quaternary ammonium ions for exchange resin for anions which is as follows: $[Fe(CN)_6]^{3-} > SO_4^{2-} > CCl_3COO^- > SCN^- > ClO_4^- > I^- > NO_3^- > CF_3COO^- > Br^- > Cl^-$. Anions of their respective salts shield the electrostatic repulsion which is the cause of protein unfolding at low pH, by directly binding to the positive charges present on the protein at low pH, resulting in the manifestation of hydrophobic interactions, favoring folding of the unfolded protein. As the concentration of salt is increased, it acts as source of anions resulting in screening of the repulsive effect between positively charged groups present on protein, thus overcoming charge–charge repulsion, causing a collapse to the molten globule state. This mechanism can be interpreted as N ↔ U ↔ salt-induced transitions, where N indicates the native state, U indicates the TCA-induced state, and salt-induced intermediate state, which can be characterized as partially refolded with the retention of secondary and partial tertiary structure.

Tryptophan fluorescence. Varying concentrations of salts, i.e., KCl, $KClO_4$, K_2SO_4, and $K_3[Fe(CN)_6]$, were taken to determine the effect of their anions on the TCA-induced state of Cyt *c*. The required concentration of salts in bringing about the structural changes varied greatly among the salts. A quenched fluorescence intensity in all the salts studied was obtained; quenching was maximum in case of $K_3[Fe(CN)_6]$ followed by K_2SO_4, $KClO_4$, and KCl (see Table 2). Since the tryptophan fluorescence in native Cyt *c* is initially found to be quenched, addition of salts to the TCA-induced state of Cyt *c* (enhanced fluorescence intensity) leading to quenching of tryptophan fluorescence, is suggestive of refolding. This agrees well with the near-UV CD data.

ANS (extrinsic) fluorescence. Changes in ANS fluorescence are frequently used to detect non-native, intermediate conformations of globular proteins [37]. On increasing the concentration of salts, the ANS fluorescence intensity increases for all salts, suggesting conformational changes in the TCA-induced state of Cyt *c* leading to the exposure of hydrophobic regions of the protein molecule as well as increase in hydrophobic interactions. Among the salts studied, $K_3[Fe(CN)_6]$ was most effective in inducing the transition. The effectiveness of various salts follows the order: $K_3[Fe(CN)_6] > KClO_4 > K_2SO_4 >$ KCl (see Table 2). The order was consistent with the order of salts in inducing the structural changes as studied by CD measurements (see Fig. 4 and Table 1).

Effect of alcohols on TCA-induced state of Cyt *c*. *CD measurements.* Figure 5 indicates the observed changes in far-UV CD and near-UV CD regions on the TCA-induced state of Cyt *c* in the presence of various alcohols at their maximum respective concentration, i.e., methanol (14 M; curve *2*), ethanol (12 M; curve *3*), propanol (11 M; curve *4*), and butanol (9 M; curve *5*). As can be seen from Fig. 5a, there was induction of secondary structure on the addition of alcohols on the TCA-induced state. Butanol induced maximum changes in the CD spectrum (curve *5*). The midpoint of transition (C_m) calculated for methanol was 10.7 M, which was much higher compared to that of butanol (3.5 M). This shows that butanol (curve *5*) was much more effective than methanol (curve *2*) in inducing secondary structure. A summary of the respective maximum MREs in the presence of alcohols, their C_m values, and percent α-helix is given in Table 1. The maximum structural changes in the near-UV CD regions (Fig. 5b) are attained in the presence of butanol (curve *5*) followed by propanol (curve *4*), ethanol (curve *3*), and methanol (curve *2*). This indicates that hydrophobic interactions between the side chains of amino acids are increasing and hence resulting in compact state. The maximum ellipticity induced by various alcohols was found to be different depending on the alkyl group. Butanol possesses a nonpolar alkyl group that strengthens intramolecular hydrogen bonds because of its ability to decrease the dielectric constant of the solvent. Further increase in the alcohol concentration beyond that at which maximum ellipticity was observed lead to protein precipitation.

Tryptophan fluorescence. There was an increase in fluorescence intensity with increase in the concentration of respective alcohols. Since the polarity of the medium decreases with increase in alcohol concentration, the dielectric constant is lower than that of the TCA environment. Hence, the nonpolar solvent induces conformational alterations in the TCA-modified Cyt *c* resulting in the increase in fluorescence intensity (see Table 2).

ANS (extrinsic) fluorescence. It should be noted that organic solvents change the properties of the environment; therefore, to avoid anomaly, a proper blank was made for every point. On increasing the alcohol concentration the ANS fluorescence intensity increases for all alcohols, suggesting conformational changes in the TCA-induced state of Cyt *c* leading to the exposure of hydrophobic regions on the protein molecule as well as increase in hydrophobic interactions. All the alcohols induced a transition from the TCA-induced to the alcohol-induced state characterized by high ANS binding. Among all the alcohols studied, butanol was found to be most effective in inducing the transition. The TCA-induced state of Cyt *c* in the presence of butanol opened more hydrophobic regions as compared to native and the TCA-induced state of the protein, making them available for ANS binding. This suggests that Cyt *c* attains molten globule-like conformation in the presence of TCA and butanol (see Table 2). Thus the effectiveness of alcohols in inducing the above transition may be said to follow the following trend: butanol > propanol > ethanol > methanol. The order was consistent with the order of alcohols in inducing the transition studied by CD measurements (see Fig. 5 and Table 1).

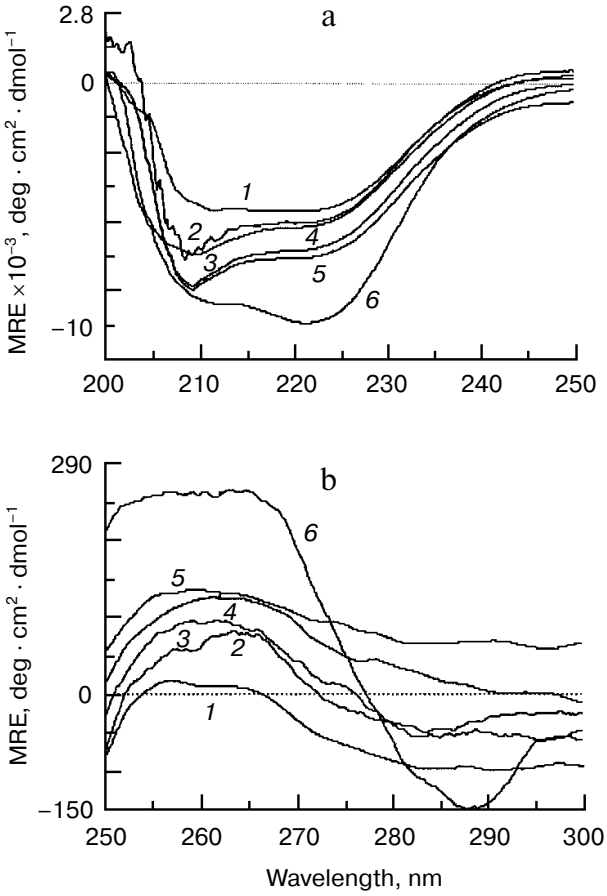

Fig. 5. Effect of alcohols on the TCA-induced state of Cyt *c*. Far-UV CD spectra (a) and near-UV CD spectra (b) of Cyt *c* in the presence of 3.3 mM TCA (curve *1*) and at the respective maximum concentration of alcohols, i.e., 14 M methanol (curve *2*), 12 M ethanol (curve *3*), 11 M propanol (curve *4*), 9 M butanol (curve *5*), and native protein (curve *6*). Protein concentration was 26 (a) and 50 μM (b) and pathlength was 0.1 (a) and 1 cm (b).

GdnHCl stability studies. To check the structural properties of the above obtained partially folded state, GdnHCl denaturation studies of Cyt *c* were performed. The fraction of protein denatured (f_D) in the presence of various cosolvents with increase in GdnHCl denaturation was calculated. The f_D of Cyt *c* in the presence of different cosolvents was calculated taking Cyt *c* individually in the presence of cosolvents at 0 M GdnHCl as the native point. Salts had a more stabilizing effect on the protein as the calculated C_m was 3 M GdnHCl concentration as compared to polyols (C_m 2.7 M) and alcohols, where C_m 2.2 M was obtained. In the presence of the above-men-

tioned cosolvents, all the transitions were single-step, two-state, and weakly cooperative. The weakly cooperative unfolding was indicative of partially folded-like nature. The fractional denaturation was least in salts followed by polyols and alcohols (data not shown).

DISCUSSION

Our far-UV CD data show the retention of secondary structure for the TCA-induced state of Cyt *c* in the presence of alcohols, polyols, and salts. In salts and alcohols, there was a regain of signal in the near-UV CD region, and some side chains were inferred to be constrained by inter-helix interactions with partial regain of tertiary structure. In the presence of polyols, there was induction in secondary structure compared to the TCA-induced state, with the loss of tertiary structure. For PEGs more secondary structure was retained in PEG-400 than in PEG-200. This can be attributed to the greater number of OH groups as the effect of polyols increases with increasing concentration and number of OH groups [32]. Fluorescence data showed increased tryptophan fluorescence intensity in case of alcohols and polyols while quenched spectra were obtained in the case of salts. There was also strong ANS binding in alcohols and polyols as well as in the presence of salts as the hydrophobic residues get exposed in this partially folded intermediate. This suggests that all the three cosolvents lead to the formation of molten globule states of Cyt *c* with different characteristics. The intermediate obtained with TFA-unfolded Cyt *c* in the presence of salts and alcohols is different from that obtained on the TCA-induced state of Cyt *c* [28]. Unlike the effect of salts and alcohols on the TFA-unfolded state, the TCA-induced state of Cyt *c* showed retention of non-native-like spectral features in the near-UV CD spectra in the presence of salts and alcohols. A summary of comparison of the respective maximum concentration of most effective salt and alcohol on TFA-unfolded and TCA-induced state is given in Table 3.

In the present study, Cyt *c* in the presence of TCA showed retention of secondary structure and more ANS binding than that at pH 2.0. In the presence of polyols, there was regain in secondary structure but loss of signal in the near-UV CD spectra. This implies that the presence of polyols results an increase in hydrogen bonding and hydrophobic interactions, leading to a compact state. Addition of alcohols leads to increase in MRE value at 208 and 222 nm, with the restoration of partial tertiary structure. In the case of salts, there was induction of secondary as well as tertiary structure with high ANS binding.

Thus, in presence of salts and alcohols, there was increase in hydrogen bonding and hydrophobic as well as inter-helix interactions. And in the presence of polyols a molten globule exists with secondary structure and high ANS binding. In the case of salts and alcohols, a state is obtained with secondary and tertiary structure as well as high ANS binding. This state can be characterized as a molten globule state. "Molten globule" (MG) is a partially structured protein folding intermediate that adopts a native-like overall backbone topology in the absence of extensive detectable tertiary interactions. Retention of tertiary structure was reported earlier for α-lactalbumin [39], RNase H [40], myoglobin [41], and ubiquitin [42].

Comparison of the intermediate states obtained to those reported in earlier work. Goto and collaborators [8, 9] have earlier reported the A-state induced by HCl with a Soret absorption maximum at 397 nm; the A-state induced by KCl with a maximum at 400 nm, and the U_A-state (acid unfolded) with a maximum at 394 nm as compared to native (412 nm). The transitions measured by the absorption change at 394 nm were consistent with the transitions measured by CD at 222 nm. However, in this paper the salt-induced state has a Soret absorption maximum at 404 nm but with almost the same extent of α-

Table 3. Comparison of different spectral properties of the TFA-induced and TCA-induced states of Cyt *c* in the presence of butanol and $K_3[Fe(CN)_6]$

Variable	TCA-induced butanol state	TCA-induced $K_3[Fe(CN)_6]$ state	TFA-induced butanol state	TFA-induced $K_3[Fe(CN)_6]$ state
MRE at 222 nm	–7.410	–7.771	– 9.120	–7.111
MRE at 262 nm	207	249	–	–
Intrinsic fluorescence intensity	136	24	142	17
λ_{max}	340	339	342	334
ANS fluorescence at 480 nm	143	59	132	15

helix induction at 222 nm (16% for salt-induced state as compared to 31% for HCl induced A-state). The C_m value of KCl was found to be 35 against 48 mM as reported earlier [8, 9]. The native tertiary structure for A-state has also been reported [43-45]. In our studies, this is due to less loss in the secondary structure of TCA-unfolded Cyt *c* as compared to pH 2.0 and hence easily attainable secondary structure at low concentration of KCl. Altogether, it can be concluded that the salt-induced state obtained in the presence of anions is different from the A-state as reported earlier.

The authors thank Dr. Syed Najmul H. Azmi, Department of Chemistry, Aligarh Muslim University, Aligarh, for his valuable suggestions. The authors thank the facilities at Aligarh Muslim University, Aligarh.

This work has also been applied for research grant in MAAS, New Delhi. The authors also thank DST-FIST for financial support. A. N. is the recipient of CSIR-SRF.

REFERENCES

1. Fink, A. L., Calciano, C. L., Goto, Y., Kurotsu, T., and Palleros, D. R. (1994) *Biochemistry*, **33**, 12504-12511.
2. Davis Searles, P. R., Morar, A. S., Saunderes, A. J., Eri, D. A., and Pielak, G. J. (1998) *Biochemistry*, **37**, 17048-17053.
3. Gekko, K., and Timasheff, S. N. (1981) *Biochemistry*, **20**, 4667-4676.
4. Freeman, W. H. (1992) in *Protein Folding* (Ptitsyn, O. B., and Creighton, T. E., eds.) N. Y., pp. 243-300.
5. Denisov, V. P., Jonsson, B. H., and Halle, B. (1999) *Nature Struct. Biol.*, **6**, 253-260.
6. Bai, P., Song, J., Luo, L., and Teng, Z. Y. (2001) *Protein Sci.*, **10**, 55-62.
7. Arai, M., and Kuwajima, K. (2000) *Adv. Protein Chem.*, **53**, 209-282.
8. Goto, Y., Takahashi, N., and Fink, A. L. (1990) *Biochemistry*, **29**, 3480-3488.
9. Goto, Y., Calciano, L. J., and Fink, A. L. (1990) *Proc. Natl. Acad. Sci. USA*, **87**, 573-577.
10. Santucci, R., Polizio, F., and Desideri, A. (1999) *Biochimie*, **81**, 745-751.
11. Santucci, R., Bongiovanni, C., Mei, G., Ferri, T. P., Polizio, F., and Desideri, A. (2000) *Biochemistry*, **39**, 12632-12638.
12. Marmorino, J. L., Lehti, M., and Pielak, G. J. (1998) *J. Mol. Biol.*, **275**, 379-388.
13. Jeng, M. F., Englander, S. W., Elove, G. A., Wand, A. J., and Roder, H. (1990) *Biochemistry*, **29**, 10433-10437.
14. Goto, Y., and Nishikiori, S. (1991) *J. Mol. Biol.*, **222**, 679-686.
15. Jordan, T., Eads, J. C., and Spiro, T. G. (1995) *Protein Sci.*, **4**, 716-728.
16. Antalik, M., and Sedlak, E. (1999) *Biochim. Biophys. Acta*, **1434**, 347-355.
17. Hamada, D., Hoshino, M., Kataoka, M., Fink, A. L., and Goto, Y. (1993) *Biochemistry*, **32**, 10351-10358.
18. Hiramatsu, K., and Yang, J. T. (1983) *Biochim. Biophys. Acta*, **743**, 106-114.
19. Dyson, H. J., and Beattie, J. K. (1982) *J. Biol. Chem.*, **257**, 2267-2273.
20. Kamatari, Y. O., Takashi, K., Kataoka, M., and Akasaka, K. (1996) *J. Mol. Biol.*, **259**, 512-523.
21. Hagihara, Y., Yukihiro, T., and Goto, Y. (1994) *J. Mol. Biol.*, **237**, 336-348.
22. Naseem, F., Khan, R. H., Haq, S. K., and Naeem, A. (2003) *Biochim. Biophys. Acta*, **1649**, 164-170.
23. Haq, S. K., Rasheedi, S., and Khan, R. H. (2002) *Eur. J. Biochem.*, **269**, 47-52.
24. Naeem, A., Khan, A., and Khan, R. H. (2005) *Biochem. Biophys. Res. Commun.*, **331**, 1284-692.
25. Kumar, Y., Tayyab, S., and Muzammil, S. (2004) *Arch. Biochem. Biophys.*, **431**, 3-10.
26. Naeem, A., and Khan, R. H. (2004) *Int. J. Biochem. Cell Biol.*, **36**, 2281-2292.
27. Naeem, A., Akram, M., and Khan, R. H. (2004) *J. Protein Chem.*, **23**, 185-195.
28. Cooper, D., and Doran, C. (1987) in *Classical Methods*, Vol. 1, John Willey and Sons, Chichester, pp. 203-282.
29. Chen, Y. H., Yang, J. T., and Martinez, H. M. (1972) *Biochemistry*, **11**, 4120-4131.
30. Tokuriki, N., Kinjo, M., Negi, S., Hoshino, M., Goto, Y., Urabe, I., and Yomo, T. (2004) *Protein Sci.*, **13**, 125-133.
31. Naeem, A., Khan, K. A., and Khan, R. H. (2004) *Arch. Biochem. Biophys.*, **432**, 79-87.
32. Kamiyama, T., Sadahide, Y., Nogusa, Y., and Gekko, K. (1999) *Biochim. Biophys. Acta*, **1434**, 44-57.
33. Stryer, L. (1968) *Science*, **162**, 526-540.
34. Ray, S. S., Singh, S. K., and Balaram, P. (2001) *J. Am. Soc. Mass-spectrometry*, **12**, 428-438.
35. Matulis, D., Baumann, C. G., Bloomfield, U. A., and Lovrien, R. E. (1999) *Biopolymers*, **49**, 451-458.
36. Matulis, D., and Lovrien, R. (1998) *Biophys. J.*, **74**, 422-429.
37. Semisotnov, G. V., Rodionova, N. A., Razgulyaev, O. I., Uversky, V. N., Gripas, A. F., and Gilmanshin, R. I. (1991) *Biopolymers*, **31**, 119-128.
38. Kuwajima, K. (1989) *Proteins*, **6**, 87-103.
39. Kataoka, M., Hagihara, Y. K., Mihara, K., and Goto, Y. (1993) *J. Mol. Biol.*, **229**, 591-596.
40. Wu, L. C., and Kim, P. S. (1998) *J. Mol. Biol.*, **280**, 175-182.
41. Khorasanizadeh, S., Peters, I. D., and Roder, H. (1996) *Nature Struct. Biol.*, **3**, 193-205.
42. Raschke, M., and Marqusee, S. (1997) *Nature Struct. Biol.*, **4**, 298-304.
43. Kay, M. S., and Baldwin, R. L. (1996) *Nature Struct. Biol.*, **3**, 439-445.
44. Marmorino, J. L., Lehti, M., and Pielak, G. J. (1998) *J. Mol. Biol.*, **275**, 379-388.
45. Marmorino, J. L., and Pielak, G. J. (1995) *Biochemistry*, **34**, 3140-3143.